CHAPTER 1
INTRODUCTION

1.1 Rational

According to the information of Thailand's Department of Alternative energy Development and Efficiency (DEDE), the statistics indicate that national energy demand in electricity form is gradually increased due to commercial floorspace continued penetration of electric appliances in the residential sector and increased of industrial output. In Thailand, the main energy resource for generating electricity is fossil fuel, accounting for 80-90% of the total energy resource. When fossil fuel is consumed, it does not only produce electricity but also emits many pollutants such as SO_x, CO, or greenhouse gases (especially CO_2). In 2000, UNFCC reported that more than half of gross CO_2 emissions of Thailand were produced from the energy supply sector. Regarding the world's environmental concern and the Kyoto protocol, these greenhouse gases must be reduced. Renewable energy together with cleaner technology is an attractive solution. At present, the alternative power technologies are developed for generating electricity from geothermal, solar, wind, and wood and waste. However, the efficiency of these technologies is still lower than the conventional technology.

Solid oxide fuel cell (SOFC) is a potentially alternative technology for power generation because it can reach 50-60% efficiency and provides relative high power density. SOFC systems can convert chemical energy directly to electrical energy for power generation. Each cell consists of a porous ceramic anode and a cathode separated by a solid ceramic electrolyte. SOFC's operate at high temperature (800-1000°C) and atmospheric or elevated pressure. According to its operating condition, the waste heat can be applied for cogeneration system. Moreover, it is flexible and able to use various primary fuels such as methane, methanol, ethanol, and other oil derivatives. These primary fuels must be converted to hydrogen-rich gas by a reformer before being fed to SOFC. It should be noted that the reformer could be placed separately or internally from a fuel cell stack, recalled "external reforming" and "internal reforming", respectively, as shown in Figure.1.1. In order to utilize the liberated heat from SOFC, the reformer is installed in the fuel cell system as called internal reforming (IR). The internal reforming of a SOFC has two approaches: Direct Internal Reforming (DIR) and Indirect Internal Reforming (IIR).

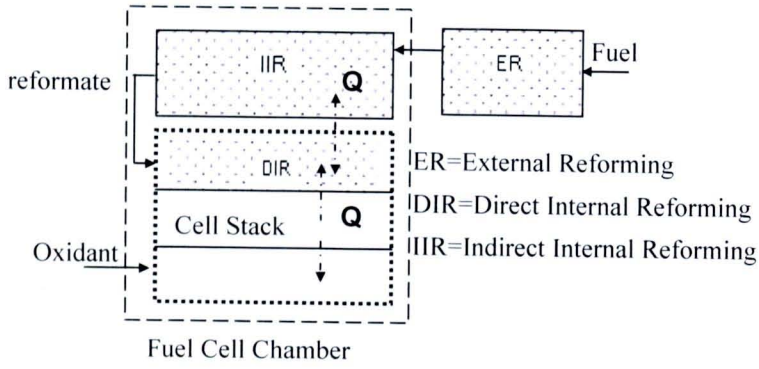

Figure 1.1 Reforming concepts for high temperature fuel cell

According to DIR operation, the reforming reaction is carried out directly at the anode. Hydrogen is generated and simultaneously consumed, resulting in high fuel conversion and more uniform temperature distribution. However, this approach suffers from two main problems. Firstly, the anode deactivation by coke formation which leads to a decrease in system efficiency. Secondly, the large temperature gradient across the cell due to the extremely endothermic reforming reaction causes a strong cooling effect, as shown in Figure.1.2. Thus, high carbon resistant and high durability are required for the anode material.

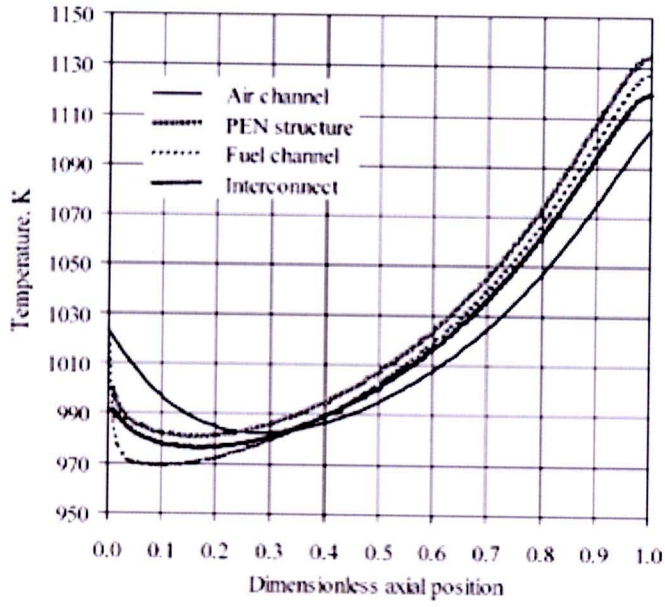

Figure 1.2 The reforming, fuel channel, and air channel temperature profiles of DIR-SOFC fueled by methane [Aguiar et al.(2004)]

Regarding IIR operation, the endothermic reforming reaction takes place at the reformer, which is in close thermal contact with the anode side of fuel cell where the exothermic electrochemical reaction takes place; this coupling process is called an autothermal operation. The main drawback of this configuration is the local mismatch between the rates of endothermic and exothermic reactions. This problem can lead to significant local temperature reduction close to the entrance of the reformer, as shown in Figure. 1.3, which can result in mechanical failure due to thermally induced stresses.

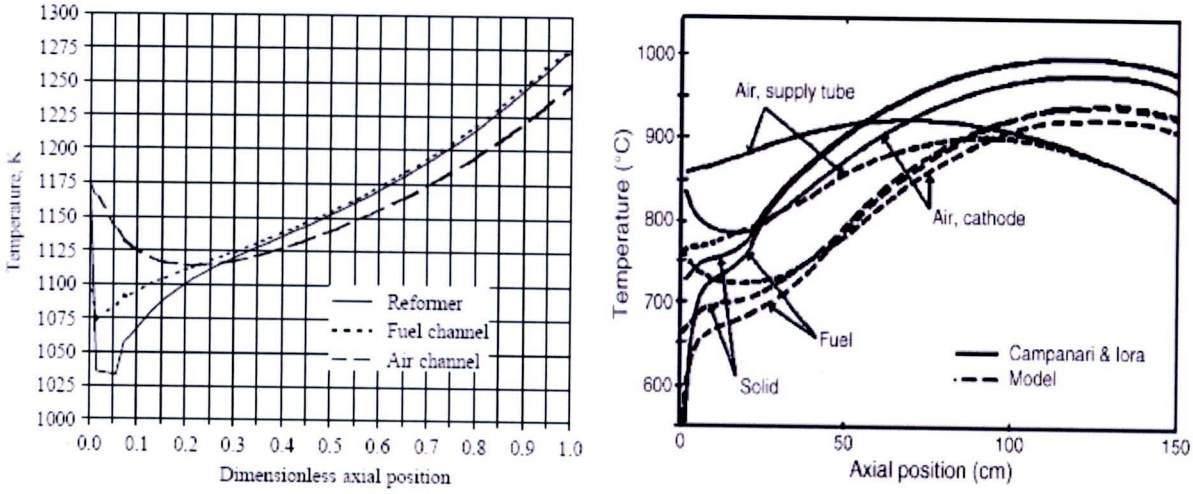

Figure 1.3 The reforming, fuel channel, and air channel temperature profiles of IIR-SOFC fueled by methane a) two-dimensional model [Aguiar et al.,(2002)], b) one dimensional model [Sanchez, 2006]

Normally, SOFCs are operated for producing electricity that should be smooth and continuous. This operating system is called Steady-State operation. The thermodynamic and kinetic properties in this operation are unchanged over time. However, steady-state operation did not occur immediately after start SOFC. SOFCs are operating at high temperature for steady state. While at ambient temperature they cannot operate at steady state then the SOFC system that must be heated to a minimum operating temperature. Operating system that occurred when operating start is called transient operation. Under this operation, the systems are changing over time (i.e., during the cell heat up to minimum cell temperature and starting up to produce electricity). Kinetic and thermodynamic properties while transient operations are changing by the time during the cell temperature changed i.e. heat-up, start-up and shutdown operation (as presented in Table 1.1).

Table 1.1 Operating process

Temperature	25°C	900°C	900°C	25°C
Operating process	Heat-up	Start up	Operating	Shut down
	Transient		Steady	Transient

1.2 Literature Review

The main objective of this research was to investigate dynamic model of indirect internal reforming SOFC. Typically, mathematical model is established for predicting the components and temperature behaviors in the system. In the case of SOFC operation, the chemical element behavior can be obtained from the kinetic rate reaction and the electrochemical analysis. Furthermore, the thermal characteristic can be acquired from thermodynamic consideration. Therefore, the previous related literatures are reviewed as the following topics: Reforming kinetic analysis and kinetic model of methane steam reforming and modeling of SOFC.

1.2.1 Kinetic Analysis and Kinetic Model of Methane Steam Reforming

During the past decade, Ni-based catalysts, such as Ni/Al_2O_3 and Ni/YSZ, are wildly unitised in methane steam reforming (MSR) process. In order to explore the impact parameter of the process, many literatures presented kinetic models with different application. The reviewed kinetic models were summarized in Table 1.2.

One of the well-known MSR kinetic models and reaction mechanism was presented by Xu and Froment (1989). They studied reactions rate of methane steam reforming, accompanied by the water-gas shift reaction, over $Ni/MgAl_2O_4$ catalyst. The intrinsic rate equations were derived based on the three significant reactions in the MSR system, as shown below.

$$CH_4 + H_2O \leftrightarrow 3H_2 + CO \quad (1.1)$$

$$CO + H_2O \leftrightarrow H_2 + CO_2 \quad (1.2)$$

$$CH_4 + 2H_2O \leftrightarrow 4H_2 + CO_2 \quad (1.3)$$

These three reactions were also concerned in the works of Hou and Hughes (2001) and Hoang *et.al.* (2005). Huo *et.al* studied the MSR kinetics over commercial $Ni/\alpha Al_2O_3$ catalysts in temperature range 748-823 K. They developed the kinetic models by using the Langmuir-Hinshelwood-Hougen-Watson assumption and Freudlich's adsorption theory. The kinetic models were reasonable fixed to the experiment data.

Table 1.2 Summary of methane steam reforming rate expressions over Ni base-catalyst

Rate Equation	Reference
$R_{CH_4} = \dfrac{k/p_{H_2}^{2.5}\left(p_{CH_4}p_{H_2O} - \dfrac{p_{H_2}^{3}p_{CO}}{k_{eq}}\right)}{(1+k_{CO}p_{CO}+k_{H_2}p_{H_2}+k_{CH_4}p_{CH_4}+\dfrac{k_{H_2O}p_{H_2O}}{p_{H_2}})^2}$	Xu and Froment,1989
$R_{CH_4} = \dfrac{k\ (T)p_{CH_4}}{\left(1+K_H(T)p_{H_2}^{0.5}+K_s(T)\,p_{H_2O}/p_{H_2}\right)^n}$	Dicks *et.al*, 2000
$R_{CH_4} = kp_{CH_4}^{\ 0.85}p_{H_2O}^{\ -0.35}$	Ahme and Foger, 2000
$R_{CH_4,1} = k_1\left(\dfrac{p_{CH_4}p_{H2O}^{0.5}}{p_{H_2}^{1.25}}\right)\left(1-\dfrac{p_{H_2}^3p_{CO}}{k_{eq1}p_{CH_4}p_{H_2O}}\right)\times\dfrac{1}{DEN^2}$ $R_{WGS} = k_{WGS}\dfrac{p_{CO}p_{H_2O}^{0.5}}{p_{H_2}^{0.5}}\left(1-\dfrac{p_{H_2}p_{CO_2}}{k_{eq,WGS}p_{H_2O}p_{CO}}\right)\times\dfrac{1}{DEN^2}$ $R_{CH_4,2} = k_2\left(\dfrac{p_{CH_4}p_{H2O}}{p_{H_2}^{1.75}}\right)\left(1-\dfrac{p_{H_2}^4p_{CO_2}}{k_{eq2}p_{CH_4}p_{H_2O}^2}\right)\times\dfrac{1}{DEN^2}$ where $DEN = 1+K_{CO}p_{CO}+K_{H_2}p_{H_2}^{0.5}+\dfrac{K_{H_2O}p_{H_2O}}{p_{H_2}}$	Hou and Hughes, 2001
$R_{CH_4,1} = \dfrac{k_1}{p_{H_2}^{2.5}}\left(p_{CH_4}p_{H_2O}-\dfrac{p_{H_2}p_{CO}}{k_{eq1}}\right)\times\dfrac{1}{Q_r^2}$ $R_{WGS} = \dfrac{k_{WGS}}{p_{H_2}}\left(p_{CO}p_{H_2O}-\dfrac{p_{H_2}p_{CO_2}}{k_{eq,WGS}}\right)\times\dfrac{1}{Q_r^2}$ $R_{CH_4,2} = \dfrac{k_2}{p_{H_2}^{3.5}}\left(p_{CH_4}p_{H_2O}^2-\dfrac{p_{H_2}^4p_{CO_2}}{k_{eq2}}\right)\times\dfrac{1}{Q_r^2}$ where $Q_r = 1+K_{CO}p_{CO}+K_{H_2}p_{H_2}+K_{CH_4}p_{CH_4}+\dfrac{K_{H_2O}p_{H_2O}}{p_{H_2}}$	Hoang *et.al.*, 2005

Due to the fact that commercial catalysts are continuously developed, Hoang *et.al.* analysed the MSR kinetics over another commercial catalyst, sulfide Ni/γAl_2O_3, in 773-1073K. Their model presented the dependency of reforming performance on temperature and

steam to carbon ration. MSR kinetic models are not only applied in the reformer, these are also utilized in the internal reforming approach for solid oxide fuel cell (SOFC) application. Dicks *et.al.* (2000) and Ahmed *et.al.* (2000) presented the MSR kinetic models which investigated over Ni/YSZ anode, in 1073 – 1173 K, with the aim of optimizing important system parameters in the DIR-SOFC. According to Dicks' model, in Table 1.1, the hydrogen partial pressure presents positive effect and negative effect of the steam partial pressure on the reaction rates. Additionally, Ahmed *et.al* (2000) presented further simplified rate equation.

Form Table 1.2, k, k_1, and k (T) are the rate constants of reaction 1.1. k_{WGS} and k_2 are the rate constants of reaction 1.2 and 1.3, respectively. k_{eq} is the equilibrium constants. K_{CH4}, K_{CO}, K_{H2} and K_{H2O} are the equilibrium constants for CH_4, CO, H_2, and H_2O adsorption respectively. p_i is the partial pressure of gas component i.

1.2.2 Kinetic Analysis and Kinetic Model of Methanol Stream Reforming

Methanol has been applied as a primary of fuel cell since the early days of fuel cell development. For methanol stream reforming, copper (Cu) is used as catalyst. Normally, reforming temperature of Cu catalysts is in the range of 433-573 K. They are always utilized in low temperature fuel cell (Ma et al., 1998). In order to use them at high temperature, the other materials are required. Until now, the kinetic rate expressions of methanol reforming were investigated over various catalyst types such as $Cu/ZnO/Al_2O_3$ (Ma *et al.*, 1998 and Peppley *et al.*1999 a,b), Mn-promoted co precipitated Cu-Al catalyst (Idem and Bakhshi,1996), Pd/ZnO (Cao *et al.*,2004) and $Cu/ZnO_2/CeO_2$ (Mastalir *et al.*, 2005). Summary of methanol steam reforming kinetic equations were presented in Table 1.3. The kinetic model of Peppley is widely applied to behaviors of predict the methanol steam reforming.

According to Peppley's rate expressions, hydrogen production from methanol was investigated within three main reactions over $Cu/ZnO/Al_2O_3$ catalysts (CZA) methanol steam reforming (MeSR), methanol decomposition (MD), and water gas shift reaction (WGS). Moreover, a comprehensive kinetic model for methanol steam reforming over CZA catalyst was applied in this study. Several researchers have previously studied the reforming mechanisms of CZA catalyst. They determined the actual kinetic rate in a fixed-bed differential reactor over a wide range of conditions. A multi-response least squares non-linear regression was used to provide the parameters for the kinetic model. The accuracy of the developed kinetic model was evaluated by comparing it with the experimental results. It was

found that the kinetic model was reliable enough to predict both the rate of hydrogen production and the composition of the production gases from the methanol steam reforming process over a CZA catalyst. It should be noted that this model was the first model of methanol steam reforming to account for all three reversible overall reactions.

Since Peppley's reaction rate was very complicated to fix in the model, Choi and Stenger developed new simplified methanol steam reforming rate expansions (Choi *et al.*, 2002). They developed methanol steam reform equations from four related reactions: methanol steam reforming, methanol decomposition, water gas shift reaction, and CO selective oxidation. These reactions were operated in a micro-reactor testing unit. The first three reactions were carried out over commercial Cu-ZnO/Al_2O_3catalysts and the last reaction was performed on Pt-Fe/γ-alumina catalysts. The reaction was operated at atmospheric pressure with temperatures between 120-325°C. The rate expressions of each reaction were achieved using non-linear least squares optimization, numerical integration of a one-dimensional plug flow reactor model, and extensive experimental data. These rate expressions were simulated and optimized to maximize profit of hydrogen yield and economic investigation using MATLAB. They were also interested in evaluating some parameters i.e. product distribution, the effect of reactor volume and temperature, and the selection of water and air feed rate. The results indicated that the most effective parameter of this simulation and optimization was the size of the reformer. Recently, Mastalier *et al.*
(2005) presented the kinetic study of MeSR over novel Cu/ZrO_2/CeO_2 (CZC) catalysts. They analyzed three important reactions of the hydrogen production from methanol according to the work of Peppley *et al.* (1999a, b). Their objectives were the structural and catalytic investigation of novel CZC catalysts and kinetic study for developing a model. Their novel CZC samples with Cu contents exceeding 5% displayed long-term stabilities and low CO levels during continuous operation.

Table 1.3 Summary of methanol steam reforming over different types of catalyst

Rate Equation	Type of catalyst	Reference
$-r_{SRM} = k_R p_{CH_3OH}^{0.263} p_{H_2O}^{0.033} p_{H_2}^{-0.20}$	$CuO/ZnO/Al_2O_3$	Jiang *et al.*, 1993
$-r_{SRM} = \frac{k_R K_{CH_3O}(p_{CH_3OH}(p_{H_2}^3 p_{CO_2} / K_R p_{H_2O}))C_{S1}C_{S1a}S_g}{(p_{H_2}^{0.5} + K_{CH_3O}p_{CH_3OH} + K_{HCOO}p_{CO_2}p_{H_2} + K_{OH}p_{H_2O})(1+K_H^{0.5}p_{H_2}^{0.5})}$ $-r_{MD} = \frac{k_{MD}K_{CH_3O(2)}(p_{CH_3OH} - (p_{H_2}^2 p_{CO_2} / K_{MD}))C_{S2}C_{S2a}S_g}{(p_{H_2}^{0.5} + K_{CH_3O(2)}p_{CH_3OH} + K_{OH(2)}p_{H_2O})(1+K_{H(2)}^{0.5}p_{H_2}^{0.5})}$ $-r_{RGS} = \frac{k_{RGS}K_{CH_3O}p_{H_2}^{0.5}(p_{CO}p_{H_2O} - (p_{H_2}p_{CO_2} / K_{RGS}))C_{S1}^2 S_g}{(p_{H_2}^{0.5} + K_{CH_3O}p_{CH_3OH} + K_{HCOO}p_{CO_2}p_{H_2} + K_{OH}p_{H2O})^2}$	$CuO/ZnO/Al_2O_3$	Peppley *et al.*, 1999
$-r_{SRM} = k_R p_{CH_3OH} p_{H_2O}$ $-r_{MD} = k_D(p_{CH_3OH} - k_{MD}^{-1} p_{H_2}^2 p_{H_2O})$ $-r_{DME} = k_{DME} p_{CH_3OH}^2$ $-r_{RGS} = k_W(p_{CO}p_{H_2} - k_w^{-1} p_{H_2}p_{CO_2})$ $-r_{MF} = k_{MF}(p_{CH_3OH})^2$ $-r_{CH_4} = k_{CH_4} p_{CH_4} p_{MF}$	$CuO/ZnO/Al_2O_3$	Choi *et al.*, 2002
$-r_{SRM} = k_R p_{CH_3OH}^{0.715} p_{H_2O}^{0.088}$	Pd/ZnO	Cao *et al.*, 2004
$-r_{SRM} = k_R p_{CH_3OH}^{0.6} p_{H_2O}^{0.4} - k_{-R} p_{CO_2} p_{H_2O}$ $-r_{MD} = k_D p_{CH_3OH}^{1.3}$ $-r_{RWGS} = k_{-W} p_{CO_2} p_{H_2} - k_W p_{CO} p_{H_2O}$	$CuO/ZnO/CeO_2$	Mastalir *et al.*, 2005

*Note: $k_R, k_D, k_{DME}, k_W, k_{MF}, k_{CH_4}$ are rate constant for MeSR, MD, DME, RWGS, MF formation and methane formation, respective. K_i is a equilibrium constant of reaction which defined previous sentence.

1.2.3 Kinetic Analysis and Kinetic Model of Ethanol Steam Reforming

Ethanol is considered to be a good hydrogen sources for fuel cells. Mainly, bio-ethanol production is less complicated than bio-methanol. In order to increase hydrogen productivity together with limited carbon monoxide, ethanol steam reforming (ESR) has been used. Though ESR had been studied during the last decades, the kinetic model was not proposed until 2006. ESR kinetic models have been recently published from two research groups: Akande *et al.* (2006) and Sahoo *et al.* (2007). These two models are summarized in Table 1.3. Akande *et al.* investigated the ESR kinetic reactions on 15% wt. Ni/Al2O3 at 593-793 K. Five kinetic models were developed based on different concepts. The first four models were derived from the Eley-Rideal mechanism. Four rate-determining steps over a catalyst active site were assumed. The last kinetic model was developed by the collected experiment data. Moreover, these five kinetic models were fixed in to the mathematic model which developed by Aboudheir *et al.* (2006). They developed the two dimensional non-isothermal model to simulate the ESR behavior in a packed bed tubular reactor. Another ESR rate expression was proposed by Sahoo *et al.* (2007). They studied the kinetic of ESR over Co/Al_2O_3 catalyst in the range of 673-973 K. Although hydrogen can be produced via several pathways in the ESR system, the only three major reactions are:

Ethanol steam reforming (ESR): $C_2H_5OH + 3H_2O \leftrightarrow 6H_2 + 2CO_2$ (1.4)

Ethanol decomposition (ED): $C_2H_5OH \leftrightarrow H_2 + CO + CH_4$ (1.5)

Water gas shift reaction (WGS): $CO + H_2O \leftrightarrow H_2 + CO_2$ (1.6)

Their kinetic model was based on Langmuir-Hinshelwood's approach. Their predicted results matched the measured results.

1.2.4 Modeling of SOFC

Mathematical simulation is one attractive way to study the fuel cell system over the past decades. In the early stage of fuel cell modeling, the simulation was developed in the isothermal-transient condition assumption. In order to achieve the real behavior of the fuel cell system, the mathematical equations become more complex by developing under non-

isothermal transient condition assumption. Moreover, operating time also affected the system behavior. There the dynamic model was also recognized.

Table 1.4 Summary of Ethanol steam reforming system over different type of catalyst

Rate Equation	Reference
$R_{ESM} = \frac{k_1 N_{EtOH}}{(1+3.83\times10^7)^2}$	Akande *et al.*, 2006
$R_{ESM} = k_r K_{CH_3CH_2^*}\left(\frac{p_{EtOH}}{p_{H_2}^{0.5}}\right)\left(1-\frac{p_{CO_2}^2 p_{H_2}^4}{K_r^* p_{EtOH} p_{H_2O}^2}\right)\times\frac{C_a^{T^2}}{DEN}$ Where $K_r^* = \frac{K_{CH_3CH_2O^*}(k_r/k_{-r})}{K_{CH_3CHO^*} K_{H_2^*}}$ $R_{ED} = k_D K_{CH_3CHO^*}\left(\frac{p_{CO_2}^2 p_{H_2}^3}{p_{H_2O}^2}\right)\left(1-\frac{p_{H_2O}^2 p_{CH_4} p_{CO_2}}{K_D^* p_{CO_2}^2 p_{H_2}^3}\right)\times\frac{C_a^{T^2}}{DEN}$ Where $K_D^* = \frac{K_{CH_3CHO^*}(k_D/k_{-D})}{K_{CH_4^*} K_{CO^*}}$ $R_{WGS} = k_{WGS} K_{HCOO^*} p_{CO_2}\left(1-\frac{p_{H_2O} p_{CO}}{K_w^* p_{H_2} p_{CO_2}}\right)\times\frac{C_a^{T^2}}{DEN}$ Where $K_W^* = \frac{K_{HCOO^*}(k_W/k_{-W})}{K_{OH^*} K_{CO^*}}$ Where $DEN = 1 + K_{CO_2^*} p_{CO_2} + K_{CO^*} p_{CO} + K_{CH_4^*} p_{CH_4} + K_{HCOO^*} p_{CO_2} p_{H2}^{0.5}$ $+K_{H_2^*} p_{H_2}^{0.5} + \frac{K_{CH_3CHO^*} p_{CO_2}^2 p_{H_2}^5}{p_{H_2O}^3} + \frac{K_{CH_3CH_2O^*} p_{EtOH}}{p_{H_2}^{0.5}} + \frac{K_{OH^*} p_{H_2O}}{p_{H_2}^{0.5}}$	Sahoo *et al.*, 2007

*Note: k_r, k_D, k_{WGS} are reaction rate of ERS, ED and WGS reaction, respectively. K_i is the equilibrium rate of reaction

In 1992, the non-isothermal model for tubular SOFC was established by Hirano *et al.* (1992). Structure and dimension of the cell in this calculation were based on the product of Westinghouse Electric Corporation. Two SOFC systems were investigated in their work i.e. conventional and fuel recycling systems. In conventional system, air was fed into the tube on the inside of the cell and the outside was exposed to the fuel gas. Heat was

exchanged between the cell, air and fuel channel. The residual air and fuel gases were burnt at the outlet of the stack but these waste gases were recovered to utilize in the fuel recycling system. Gases and temperature profiles were concerned only along z-axial of tube.

In addition, a planar SOFC system was then simulated by Achenbach. (1994). Three-dimension and time-dependent effects were concerned in this model. Methane and steam were fed into system. All gases behaviors were kinetically controlled. The consequence of the conduction, convection, and radiation heat transfer were accounted in the thermodynamic model. In electrochemical calculation, they developed the equations in order to calculate the resistances of electrodes. Although these equations were not confirmed by reliable experiment, it had been applied in several SOFC modeling until now. The models were computed under the following conditions. Inlet gases were 1173 K, the cell was carried out at 1 bar with 85% fuel utilization, and current density was fixed at 3000 A/m^2. The effects of difference flow patterns (cross-, co-, or counter- flow) were examined by setting boundary conditions. The simulation results showed that counter-flow provided the highest cell efficiency with uniform current density distributions. In contrast, the large temperature gradient, which is the major problem of indirect configuration, occurs for cross-flow model, as shown in Figure 1.4.

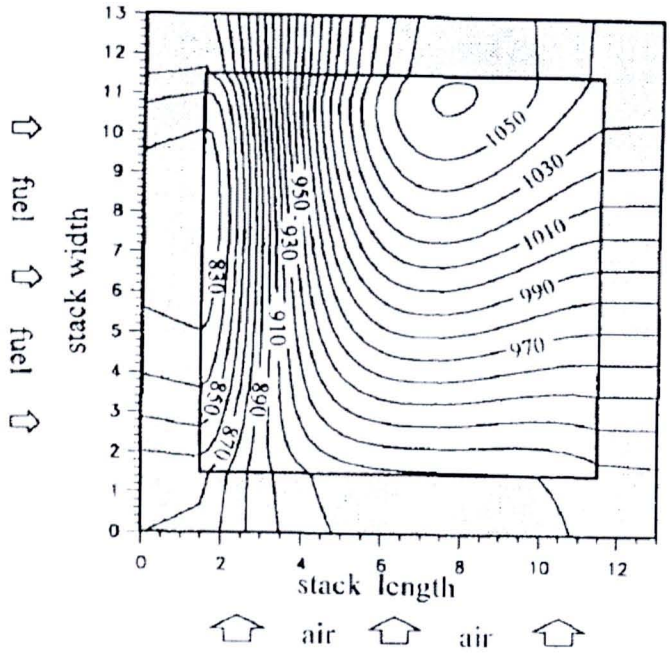

Figure 1.4 Temperature of the planar solid electrolyte for cross-flow pattern [Achenbach, 1994]

Ma *et al.* (1996) simulated the methanol reforming in an autothermal reactor. They concerned with the combination of three main reactions; methanol oxidation, MeSR, and WGS reaction. One-dimensional mathematic models were developed to investigate the performance of a class of adiabatic dual-bed catalytic reactor systems with cylindrical and spherical geometries, as shown in Figure 1.5. In their simulation, intraphase and interphase transport in porous media was neglected; therefore, the temperature and conversion profiles are determined by kinetics and reactor geometry. The kinetic equation of methanol SR was specific for CuO-ZnO-Al_2O_3 catalysts that were employed in this work. It should be noted that the optimum conditions for Cu-based catalysts are 433-573 K. These catalysts were sintered beyond 573 K and inactive at temperature lower than 433 K. The models were solved using a fourth-order Runge-Kutta numerical integration technique. The simulation results show that the spherical reactor - the Pt-Al_2O_3 catalyst was in the inner sphere - might be the most optimal geometry. The coaxial double-pip design was portable for the small reactor volume. The annular oxidation bed is a more costly preferable process.

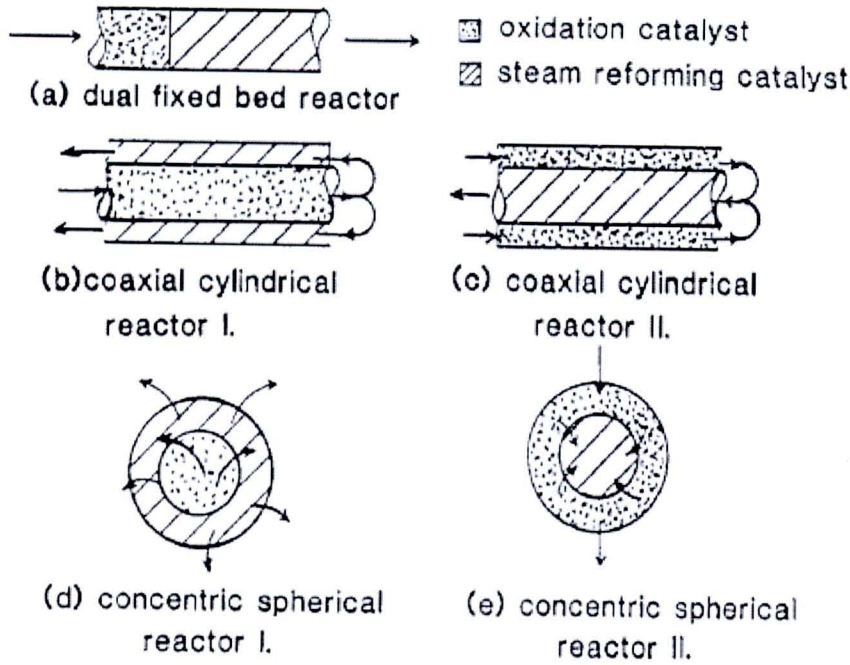

Figure 1.5 Autothermal reactor schemes [Ma.et.al, 1996]

Aguiar *et al.* (2002) presented the modeling of indirect internal reforming SOFC based on the calculation work from Park *et al.* (2002). Although SOFCs configuration has several possible designs, this study was based on a simple generic annular design where

the cell structures are assembled around a tubular packed-bed reforming reactor using typical metal-based catalysts. They provided two coupled models: two-dimensional steam reforming packed-bed reactor and a one-dimensional SOFC one. These two models were used to investigate the mismatch between the thermal load associated with the steam reforming rate and the local quantity of heat available from the fuel cell reactions, as shown in Figure 1.3 a. Moreover, they applied these models to simulate temperature, composition and related electrochemical variables along the reformer and the cell stack in order to investigate the change in some of the parameters: catalyst activity, fuel inlet temperature, current density and operating pressure. They observed that the increase of the operating pressure reduces the mismatch of heat requirement of the reformer and heat generation from the fuel cell and raise the overall temperature across the cell.

For IIR-SOFC tubular design was recently proposed by Sánchez *et.al.* (2006). The two dimensional non-isothermal model was derived to simulate the temperature distribution along the tubular IIR-SOFC under methane steam reforming system. Two new ideals were considered in their model. Firstly, the equilibrium theory was concerned to predict concentration profile. Another new ideal was gray gas radiation in the anode side. This was added into radiation heat transfer calculation. Moreover, they tried to omit the simulation errors which mainly result of simplified equations of three major overpotentials: activation, ohmic, and concentration. Thus, Butler-Volmer equation was used to calculate activation loss. Fick's law model was concerned in concentration loss computation. Ohmic loss was calculated from the correlation of temperature, current, and properties of cell materials. Since it is impossible to collect data for temperature profile along the tube, their simulation results were validated with the computed results of Campanari and Iora (2004), as shown in Figure 1.4 b. The cooling effect still appeared at the initial of the IIR-SOFC.

Decreasing of fuel utilization was negative effect on temperature distribution

Transient model are presented in many researches, David J. Hall *et. al* (1999) simulated the transient operating of a tubular solid oxide fuel cell (SOFC) which includes electrochemical thermal and mass transfer output. Figure 1.6 shown effect of the load change on inlet cell maximum temperature (1169 K) and minimum temperature (1059 K).

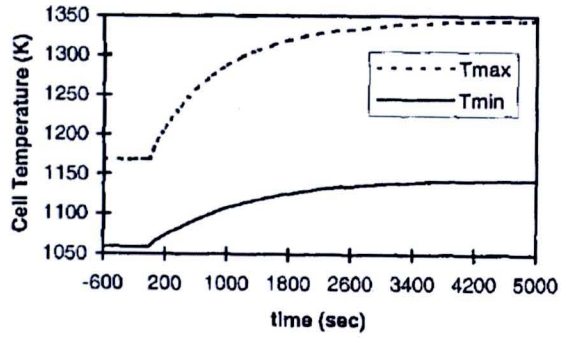

Figure 1.6 Cell Temperatures during a load change [David J. Hall et. al, 1999]

Recently, the effect of heat/mass transfer and electrochemical reaction of dynamic modeling of single tubular SOFC was developed by X. Xue *et al.* (2005). This model is studied in steady state and transient behavior. The polarization performance and output power density are determined by a variety of interacting fuel cell state variables such as fuel/gas partial pressure distribution, heat transfer between cell body and gases shown in Figure 1.7. Due to the non-uniform distribution of the Nernst potential along the longitudinal direction, the external load voltage plays an important role in the cell performance. When the Nernst potentials of some segments of the fuel cell are lower than the external load voltage, these segments will not be able to contribute current. A series of experimental and numerical studies are carried out to verify the model and explore the underlying dynamic behavior. This model can be readily used in system optimization and dynamic control.

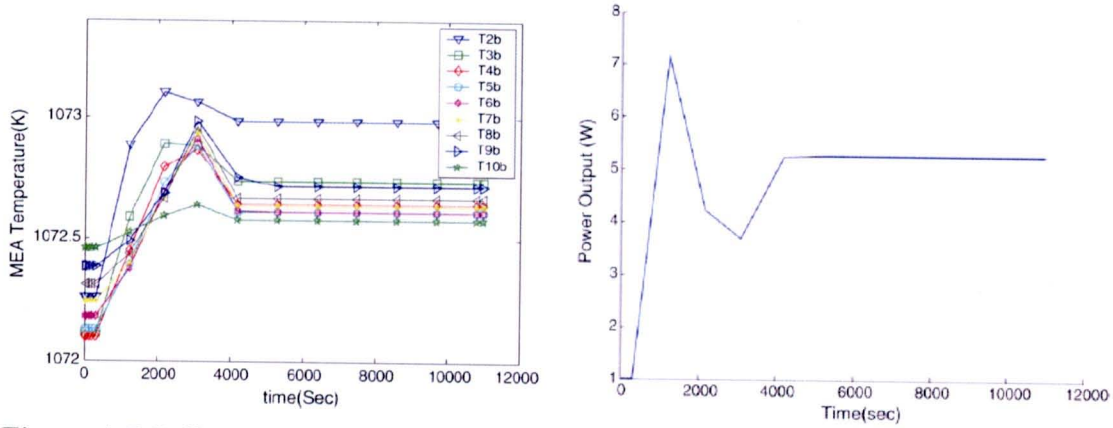

Figure 1.7 Cell Temperature distribution transient response and Fuel cell output power [X. Xue *et. al*, 2005]

During transient process, one of most interesting parameters is thermal stresses. Mustafa Fazil Serincan et.al (2010) simulated thermal stresses in an operating micro-tubular solid oxide fuel cell with COMSOL. Thermal stresses are the main factors for the failure of SOFC material. They studied the failure of each component of SOFC i.e. Anode (Ni, GDC and LSCF), Electrolyte, Cathode, Sealant and alumina tube. First calculate the residual stresses induced during sintering of the anode/electrolyte structure, taking the stress free temperature as 1450°C. Anode tends to shrink more than the structure while cooled down to room temperature shown in Figure 1.8

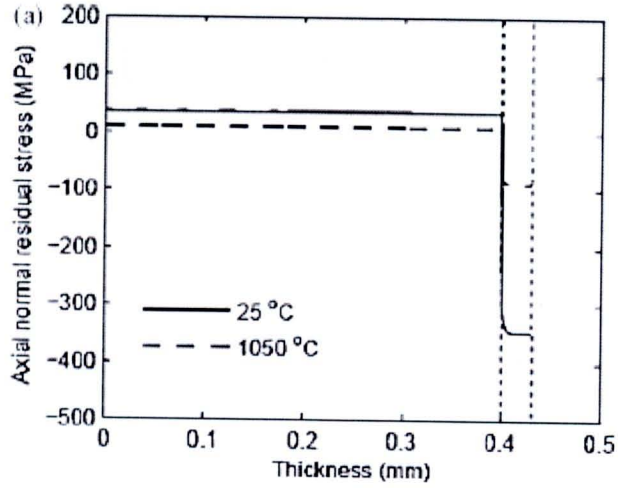

Figure 1.8 Residual stresses after the first sintering process in the anode and the electrolyte

Stress distribution in an operating micro-tubular SOFC is predicted with the calculated residual stresses given as initial stress fields. SOFC is attached to the alumina tubes with the sealant applied between the electrolyte coating and the inner surface of the tubes at room temperature. Therefore the stress free temperature for the assembly is taken as 25 ◦C as no stress is assumed to build up at the interfaces of the sealant between the cell and the tubes. However, residual stresses exist in the cell components. With the predicted temperature distribution of a micro-tubular SOFC operating at 0.7 V, thermal stresses occurring during the operation are calculated. In the actual SOFC operation, fuel is supplied to the cell as a mixture of 20 % by volume hydrogen and 80 % by volume nitrogen at a flow rate of 25cm^3 min^{-1} whereas ambient air is used at the cathode. The furnace temperature is controlled at the air channel as 550 ◦C while overpotentials cause a

higher temperature in the cell. As seen in Figure 1.9 it is predicted that the maximum temperature in the cell is 561 °C at 0.7V.

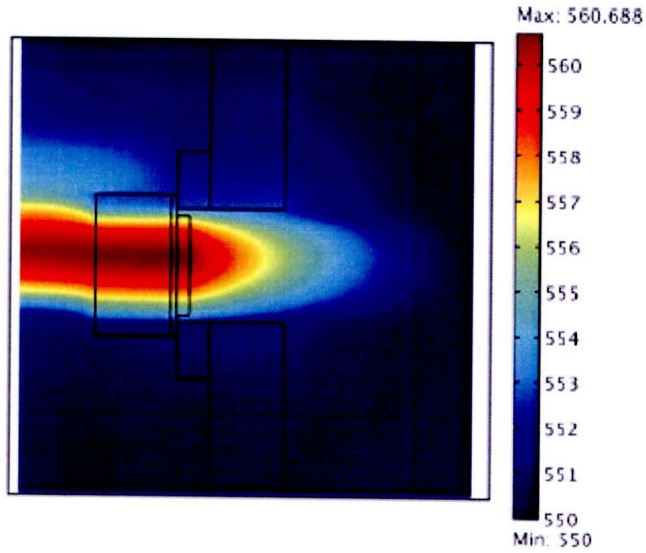

Figure 1.9 Predicted temperature distributions for the SOFC operating at 0.7 V.

For used hydrocarbon as a primary fuel of fuel cell, it should be reform to hydrogen-rich gas by reformer catalyst. IIR-SOFC application with different reformer configurations as packed-bed internal reformer and coated-wall internal reformer is shown in Figure. 1.10 and 1.11.

The benefits of coated-wall reformer with catalyst wash-coated at inside surface are excellent heat transfer characteristics and low pressure drop across the reactor. In addition, as the amount of catalyst per volume for the catalytic coated-wall reformer is lower than catalytic packed-bed reformer, this could be a great benefit for the application in IIR-SOFC, where only low methane stream conversion is required. (Dokmaingam *et al.*, 2009)

1.3 Objective

To develop the transient dynamic-model of tubular design Solid Oxide Fuel Cell with Indirect Internal Reforming operation (IIR-SOFC) fuelled by various primary fuels (i.e., methane, methanol and ethanol) during starting-up period.

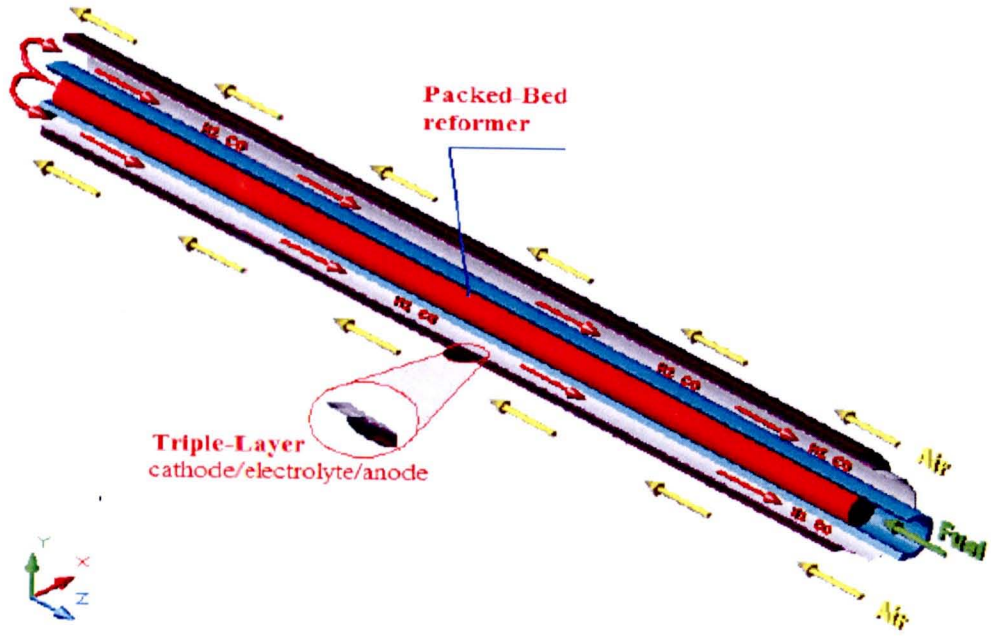

Figure 1.10 Catalytic packed-bed reactor

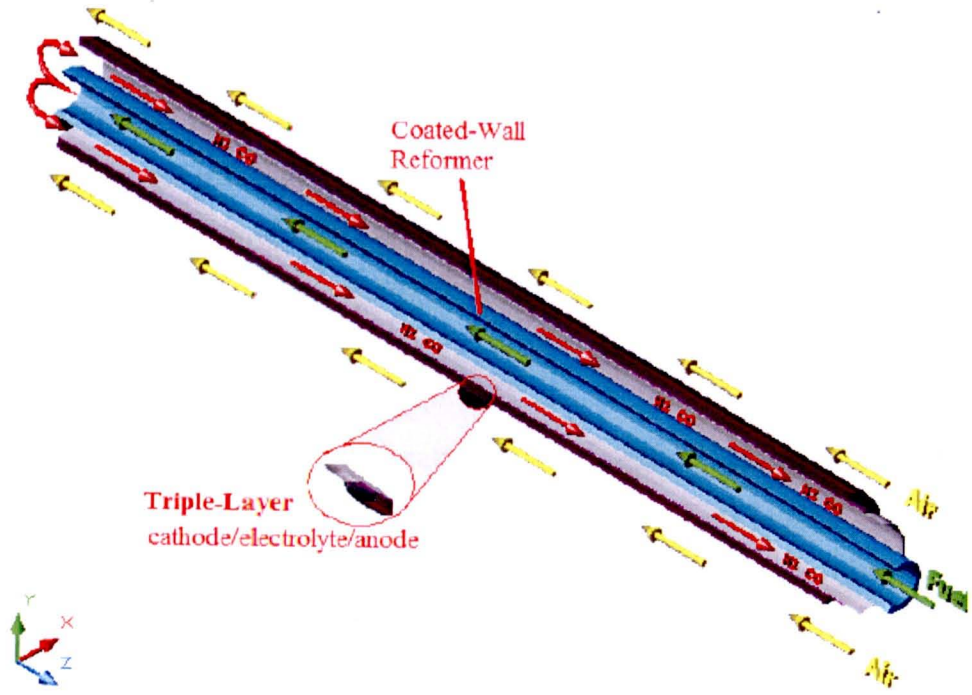

Figure.1.11 Catalytic coated-wall reactor